Mosaic length and finite interaction-range effects in a one-dimensional random energy model

2008 J. Phys. A: Math. Theor. 41 324011

(http://iopscience.iop.org/1751-8121/41/32/324011)

IOP PUBLISHING JOURNAL OF PHYSICS A: MATHEMATICAL AND THEORETICAL

J. Phys. A: Math. Theor. **41** (2008) 324011 (13pp) doi:10.1088/1751-8113/41/32/324011

Mosaic length and finite interaction-range effects in a one-dimensional random energy model

S Franz[1], **G Parisi**[2] **and F Ricci-Tersenghi**[2]

[1] Université Paris-Sud, LPTMS, UMR8626, Bât 100, 91405 Orsay cedex, France
[2] Dipartimento di Fisica, INFM-CNR SMC and INFN sez di Roma 1, Università di Roma 'La Sapienza', P.le A Moro 2, Roma 00185, Italy

Received 30 November 2007, in final form 12 February 2008
Published 30 July 2008
Online at stacks.iop.org/JPhysA/41/324011

Abstract

In this paper, we study finite interaction-range corrections to the mosaic picture of the glass transition as it emerges from the study of the Kac limit of large interaction range for disordered models. To this aim we consider point-to-set correlation functions, or overlaps, in a one-dimensional random energy model as a function of the range of interaction. In the Kac limit, the mosaic length defines a sharp first-order transition separating a high overlap phase from a low overlap one. Correspondingly, we find that overlap curves as a function of the window size and different finite interaction ranges cross roughly at the mosaic length. Nonetheless, we find a very slow convergence to the Kac limit and discuss why this could be a problem for measuring the mosaic length in realistic models.

PACS numbers: 05.20.+y, 64.70.Pf, 75.10.Nr

1. Introduction

The paradigm of 'random first-order transition', or one-step replica symmetry breaking (1RSB) theory, provides an elegant framework to conceptualize the phenomenology of liquids approaching the glass transition [1]. Unfortunately, this scenario is strongly based on mean-field models [2] and mean-field-like approximations to liquid theories [3] and cannot be taken literally in the application to real system. The main node that has to be untied to establish the 1RSB scenario as a convincing theory for real materials, is how mean-field theory should be adapted and modified to take into account the finite range of interactions. Though a fundamental theory of glassy systems in finite dimension is presently lacking, proposals have been made that modify minimally mean-field scenarios to take into account the finite interaction range. In [2], Kirkpatrick, Thirumalai and Wolynes developed a phenomenological theory, known as 'mosaic picture', where it is postulated the existence of a coherence length that grows on lowering the temperature. Below that length the system behaves essentially as a mean-field glass, while it would cross over to liquid behavior at larger scales. The result is a

theory where relaxation is dominated by activated processes stemming from the competition between interface tension and a bulk configurational entropy. The mosaic picture has been recently revived and deeply clarified by Bouchaud and Biroli [4], who showed that while usual (point-to-point) correlation functions are insensitive to the possible growth of the coherence mosaic length, it is possible to define different 'point-to-set' correlation functions, able to reveal the growth of the mosaic length. In turn, the mosaic length has been related to the relaxation time of ordinary, time-dependent correlation functions [5]. These papers prompted on one side numerical simulations on kinetically constrained glasses [6] and on realistic glassy models [7], on the other to theoretical calculations for models on trees and under the Kac limit [8]. These last models are the natural starting point for understanding the mosaic picture, since their local properties are well described by mean-field theory [9]. In [8] the study of point-to-set correlation function has allowed us to derive a detailed picture relating the relaxation in the mode coupling regime for $T > T_d$ to the one in the mosaic regime for $T < T_d$. The calculation, supposedly exact, concern the behavior of disordered glasses in the Kac limit. In order to understand its relevance for short range systems, it is necessary to study the properties of convergence to the Kac limit for finite interaction range. It has been found in [7] that in standard Lennard–Jones super-cooled liquids, the transition from high to small overlap as a function of the box size is much smoother than one would expect from the mosaic picture. This poses the question of what behavior one should expect when the range of interaction is not large.

In this paper, we address this question in a minimalistic finite-dimensional model displaying 1RSB behavior in the Kac limit. The model is a one-dimensional version of the random energy model[3] [10] extensively studied in the context of stochastic models for reaction diffusion equations and evolving populations [11]. This has two main advantages: on one hand the Kac limit can be studied directly by probabilistic arguments, without having to resort to replicas or cavity techniques, on the other the model for finite interaction range can be studied exactly by transfer matrices.

A recent paper addresses the problem of finite range corrections to the mosaic picture in a related one-dimensional XORSAT model [12]. That paper concerns the zero-temperature limit, while we concentrate on finite temperature properties.

The organization of the paper is the following. In section 2 we define the model. Section 3 is devoted to the definition of the point-to-set correlation we study. In section 4, we discuss theoretical approaches to the computation of this quantity. In section 5, we discuss the results of exact computations with transfer matrices. Finally, we draw our conclusions.

2. The model

In order to compare the behavior of finite range-interaction systems with mean-field theories, we need a model with variable interaction range which is well suited for numerical analysis. We decided to consider the 1D version of the random energy model (REM) [10] introduced in the first of [11]. This consists in a line of mL Ising spins, divided in L groups of m spins such that only neighboring groups of spins interact (thus leading to an interaction range of $2m$).

For each group $i = 1, \ldots, L$ we define a state variable σ_i taking values $1, \ldots, 2^m$. In the variables $\{\sigma_i\}$ the interactions are restricted to nearest neighbors. The Hamiltonian of the system is

$$H(\vec{\sigma}) = \sum_{i=0}^{L-1} E_i(\sigma_i, \sigma_{i+1}). \tag{1}$$

[3] The random energy model is somehow particular since it has formally $T_d = \infty$.

For each link the 2^{2m} interaction energies $E_i(\sigma, \tau)$ are quenched random variables extracted from a Gaussian distribution of zero mean and variance

$$\overline{E^2} = m/2. \tag{2}$$

We have considered fixed boundary conditions on the left side (in $i = 0$), defining $\sigma_0 = 1$, and open boundary conditions on the right side (in $i = L$). In this way, we minimize the computational effort needed to compute the free energy Z_L, which is expressed as $Z_L = \sum_\sigma Z_L(\sigma)$, where $Z_L(\sigma)$ is given by the recursion relation

$$Z_{\ell+1}(\sigma) = \sum_{\tau=1}^{2^m} Z_\ell(\tau)\, \mathrm{e}^{-\beta E_\ell(\tau,\sigma)}, \tag{3}$$

with $Z_0 = 1$ and $\beta = 1/T$. Computing Z_L thus requires $\mathcal{O}(L2^{2m})$ operations.

In the $m \to \infty$ limit, the thermodynamics is simple: the correlations between the energy level implied by the one-dimensional structure are negligible and, independently of L, the free energy coincides with the one of a REM with 2^{mL} states and energies distributed according to $P(E) \propto \exp(-E^2/mL)$:

$$F = \lim_{m\to\infty} -\frac{T}{mL} \log Z_L = \begin{cases} -\dfrac{\beta}{4} - T\log(2) & T > T_c, \\ -\sqrt{\log(2)} & T \leqslant T_c, \end{cases} \tag{4}$$

with $T_c = (2\sqrt{\log(2)})^{-1}$.

3. The observables

Here we define the correlation functions of interest, allowing us to detect a growing static length. These are built with the aid of a suitably chosen reference configuration $\{\sigma_i^*\}_{i=1,\ldots,L}$, to which one fixes the system outside a window with ℓ sites located around the center of the system. For convenience we renumber $1, \ldots, \ell$ the sites in the central window. Inside the window the system is at thermal equilibrium. We investigate the correlation among typical in-window configurations $\vec{\sigma}$ with $\vec{\sigma}^*$ to see whether a characteristic length ℓ_c exist such that for window sizes $\ell < \ell_c$, $\vec{\sigma} \simeq \vec{\sigma}^*$ inside the window, while, for $\ell > \ell_c$, $\vec{\sigma}$ and $\vec{\sigma}^*$ are uncorrelated.

As detailed in the following, in order to sharpen the transition from correlated to uncorrelated behavior we decided to fix the reference configuration $\vec{\sigma}^*$ always to the ground state. We then study the thermodynamics of a system which is fixed to the reference configuration outside a window of size ℓ:

$$\sigma_i = \sigma_i^* \qquad \forall i < 1 \qquad \text{and} \qquad \forall i > \ell. \tag{5}$$

The system has then fixed boundaries and ℓ free variables, $\{\sigma_i\}_{i=1,\ldots,\ell}$. Within the window, we can define its overlap with respect to the reference configuration as

$$q(\vec{\sigma}, \vec{\sigma}^*) \equiv \frac{1}{\ell} \sum_{i=1}^{\ell} \delta(\sigma_i, \sigma_i^*). \tag{6}$$

Note that our point-to-set correlation function differs from the one defined in [4], and used subsequently, which consists in choosing σ^* as a configuration thermalized at temperature T. We have checked that our choice makes the transition at ℓ_c sharper, and is thus more appropriate to study finite range effects.

We need some observable estimating the similarity of the typical configuration with respect to the reference one, and to this end we introduce the following two quantities:

$$p_0(\ell, \beta) \equiv \frac{\mathrm{e}^{-\beta \sum_{i=0}^{\ell} E_i(\sigma_i^*, \sigma_{i+1}^*)}}{\sum_{\{\sigma_i\}_{i=1}^{\ell}} \mathrm{e}^{-\beta \sum_{i=0}^{\ell} E_i(\sigma_i, \sigma_{i+1})}}, \tag{7}$$

$$q_0(\ell, \beta) \equiv \frac{\sum_{\{\sigma_i\}_{i=1}^{\ell}} q(\vec{\sigma}, \vec{\sigma}^*)\, \mathrm{e}^{-\beta \sum_{i=0}^{\ell} E_i(\sigma_i, \sigma_{i+1})}}{\sum_{\{\sigma_i\}_{i=1}^{\ell}} \mathrm{e}^{-\beta \sum_{i=0}^{\ell} E_i(\sigma_i, \sigma_{i+1})}}, \tag{8}$$

where the denominator is the 'window partition function'. The first quantity, p_0, is the relative weight of the reference configuration in the window partition function computed at inverse temperature β, while the second quantity, q_0, is the mean overlap with the reference configuration. Both quantities still depend on the quenched disorder and we compute their typical values by $\log(p_{\mathrm{typ}}) \equiv \overline{\log(p_0)}$ and $\log(q_{\mathrm{typ}}) \equiv \overline{\log(q_0)}$, where the overline stands for the average over the quenched disorder. We expect $\log(p_0)$ and $\log(q_0)$ to be self-averaging, since these are related to free-energy differences.

4. Theoretical analysis

In this section we address the problem of an analytic computation of the correlation functions. We will first study exactly the asymptotic long-range limit $m \to \infty$. After that we will address the problem of finite m effects that our numerical analysis below reveals to be very large.

4.1. The correlation functions for $m \to \infty$

The infinite m limit can be understood since in this limit the correlations between the energy level due to the one-dimensional structure of the model become negligible. In this case, using this independence approximation, we see that, besides the state $\vec{\sigma}^*$ of energy E^*, the window has $2^{m\ell} - 1$ states with energies distributed according to $P_\ell(E) \propto \mathrm{e}^{-E^2/m(\ell+1)}$ (there are ℓ sites and $\ell + 1$ links!). So that the average density of states is

$$\mathcal{N}(E) \sim 2^{m\ell}\, \mathrm{e}^{-E^2/m(\ell+1)} + \delta_{E,E^*} \tag{9}$$

and the microcanonical entropy per link (divided by m) as a function of the link energy $\epsilon = E/m(\ell + 1)$ is

$$S_\ell(\epsilon) = \begin{cases} -\epsilon^2 + \frac{1}{1+1/\ell} \log(2) & |\epsilon| < \sqrt{\frac{1}{1+1/\ell} \log(2)} \\ 0 & \text{otherwise.} \end{cases} \tag{10}$$

From this function the canonical thermodynamics can be derived. Before doing that, a few comments are in order: (a) the constrained entropy is reduced by a constant term with respect to the unconstrained case, given by the above formula with $\ell = \infty$ (see figure 1). (b) The choice of the reference configuration $\vec{\sigma}^*$ as the ground state has no effect on the other states: the same entropy would be obtained for different choices of σ^*. Of course the window thermodynamics and correlations would depend on the energy of $\vec{\sigma}^*$.

If the state $\vec{\sigma}^*$ was absent, the free-energy per link would read

$$\tilde{f}(\beta, \ell) = \begin{cases} -\frac{\beta}{4} - \frac{T}{1+1/\ell} \log(2) & T > T_c \sqrt{1 + 1/\ell} \\ -\sqrt{\frac{1}{1+1/\ell} \log(2)} & T \leqslant T_c \sqrt{1 + 1/\ell}. \end{cases} \tag{11}$$

Including the state $\vec{\sigma}^*$ one therefore has

$$f(\beta, \ell) = \min\{\epsilon^*, \tilde{f}(\beta, \ell)\}, \tag{12}$$

with $\epsilon^* = -\sqrt{\log(2)}$, that is the ground-state energy of the $\ell = \infty$ system. When the two terms in equation (12) are equal, a first-order transition takes place (see figure 1) at inverse

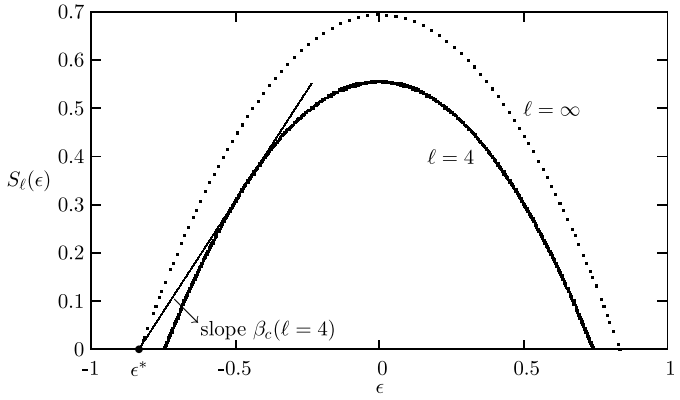

Figure 1. Microcanonical entropy for the full system ($\ell = \infty$, dotted line) and for a window of size $\ell = 4$ (thick line). A system prepared in the ground state of the full system (big dot) and constrained in a window of size $\ell = 4$ makes a first-order transition at inverse temperature $\beta_c(\ell = 4)$ (the slope of the thin line).

temperature,

$$\beta_c(\ell) = 2\sqrt{\log(2)}\left(1 - \frac{1}{\sqrt{\ell+1}}\right) = \beta_c\left(1 - \frac{1}{\sqrt{\ell+1}}\right), \tag{13}$$

which in turn defines a temperature-dependent critical length,

$$\ell_c(\beta) = \frac{\beta(2\beta_c - \beta)}{(\beta_c - \beta)^2}, \tag{14}$$

separating the confined regime $\ell < \ell_c$ where $p_{\rm typ} = q_{\rm typ} = 1$ from the deconfined regime $\ell > \ell_c$ where $p_{\rm typ} = q_{\rm typ} = 0$.

The size of the critical window diverges as expected at the critical temperature, where the configurational entropy vanishes. We find that this critical length is quadratic in the inverse of $T - T_c$; had we chosen the reference state $\vec{\sigma}^*$ with a different rule, the result would have been different. For example, a direct calculation shows that choosing $\vec{\sigma}^*$ with Boltzmann probability at temperature T implies a linear critical length in $1/(T - T_c)$.

We can understand better the structure of the excitations studying the window free-energy as a function of the overlap q, i.e. the free energy of configurations that do not coincide with $\vec{\sigma}^*$ on exactly d sites among the ℓ of the window, with $q = 1 - d/\ell$. For simplicity, we can consider the contribution of 'one bubble configurations' where all the d sites in question are contiguous. We show below that configurations with more than one bubble are exponentially improbable for large m values.

For large m, the dominant contribution to the free-energy per link $f(\beta, \ell, d) = \lim_{m\to\infty} F/m(\ell+1)$ is independent of the position of the bubble and reads, for $d = 1, \ldots, \ell$,

$$f(\beta, \ell, d) = \begin{cases} -\frac{\ell-d}{\ell+1}\sqrt{\log(2)} - \frac{d+1}{\ell+1}\left(\frac{\beta}{4} + \frac{T}{1+1/d}\log(2)\right) & T > T_c\sqrt{1+1/d}, \\ -\frac{\ell-d}{\ell+1}\sqrt{\log(2)} - \frac{d+1}{\ell+1}\sqrt{\frac{1}{1+1/d}\log(2)} & T \leqslant T_c\sqrt{1+1/d}. \end{cases} \tag{15}$$

For $d = 0$ the free energy is simply given by $f(\beta, \ell, 0) = \epsilon^*$. As one can explicitly see, f is monotonically decreasing in d: the completely open configuration is always the most favored among the ones with $d \geqslant 1$. Note that at low temperature $f(\beta, \ell, 1) > f(\beta, \ell, 0)$, and the difference $B(\beta) = (l+1)[f(\beta, \ell, 1) - f(\beta, \ell, 0)]$ can be interpreted as a relaxation

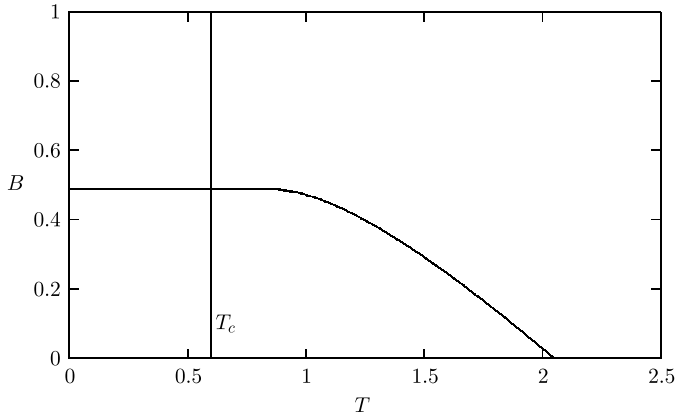

Figure 2. The free-energy barrier to relax from the ground state $\vec{\sigma}^*$.

free-energy barrier for a system prepared in the ground state $\vec{\sigma}^*$. The barrier $B(\beta)$, plotted in figure 2, is ℓ-independent and vanishes at a temperature $T = T_c/(1 - 1/\sqrt{2})$.

If we remove the assumption of considering only one-bubble configurations, the free energy in equation (15) becomes

$$f(\beta, \ell, d) = \min_{b \in \{1, d/2\}} f(\beta, \ell, d, b), \tag{16}$$

where $f(\beta, \ell, d, b)$ is the free energy of configurations differing in d variables from $\vec{\sigma}^*$ and having b bubbles, given by the following expression in the large m limit:

$$f(\beta, \ell, d, b) = \begin{cases} -\frac{\ell+1-d-b}{\ell+1}\sqrt{\log(2)} - \frac{d+b}{\ell+1}\left(\frac{\beta}{4} + \frac{T}{1+b/d}\log(2)\right) & T > T_c\sqrt{1+b/d}, \\ -\frac{\ell+1-d-b}{\ell+1}\sqrt{\log(2)} - \frac{d+b}{\ell+1}\sqrt{\frac{1}{1+b/d}\log(2)} & T \leqslant T_c\sqrt{1+b/d}. \end{cases} \tag{17}$$

It is easy to verify that the minimum in equation (16) is always achieved in $b = 1$, i.e. on one-bubble configurations. Multi-bubble configurations can only modify the corrections to the leading behavior in m.

We would like to end this section commenting that, although this paper concerns the 1D case, the analysis presented here for $m \to \infty$ generalizes to arbitrary dimension [13] where they give results in agreement with [8]. For arbitrary dimensions, the behavior of the critical length depends on the choice of σ^* and behaves as $1/(T - T_c)^2$ if σ^* is the ground state and as $1/(T - T_c)$ if σ^* is a thermalized state at temperature T. Correspondingly, the interfaces are flat, and form manifolds of dimension $\theta = d - 1$.

4.2. Analysis of the ground state

We would like to present here some attempts to take into account finite m contributions. Corrections to the asymptotic result have two sources: the correlations between the levels and sample-to-sample fluctuations. Though we were not able to deal with the former, we could analyze some of the latter.

Actually, we derive some analytical results under two main approximations, namely (i) energy levels are basically treated as uncorrelated and (ii) the energy of the reference configuration (the ground-state energy E^*) is considered to be evenly distributed among the links, each one having a local energy $m\epsilon^* = E^*/L$ (please note that the entire system is made

of L links, while the window had $\ell + 1$ links). We will see below that numerical evidence shows that this is the case not too close to the boundaries $i = 0$ and $i = L$.

The distribution of ϵ^* is known for $L = 1$, since in that case $m\epsilon^*$ corresponds to the minimum among 2^m independent random Gaussian variables of variance $m/2$, that is

$$\epsilon^*(L=1) \stackrel{\mathrm{d}}{=} -\sqrt{\log(2)} + \frac{\log(m) + \log(4\pi\log(2)) + 2X}{4m\sqrt{\log(2)}} + \mathcal{O}\left(\frac{\log(m)}{m^2}\right), \tag{18}$$

where X is a Gumbel distributed variable, i.e. $\mathbb{P}(X > x) = \mathrm{e}^{-\mathrm{e}^x}$. Similarly, a closed formula can be obtained for $L = 2$ which corresponds to a two-level GREM. Unfortunately, as soon as $L > 2$ there are no exact results on the ground-state energy of the model. In this case, an analytical upper bound can be simply constructed by the following greedy algorithm: given that σ_0 is fixed, assign σ_1 to the value minimizing $E(\sigma_0, \sigma_1)$ and repeat the procedure recursively on the next variable; at each step the link energy has the same probability distribution as $m\epsilon^*(L = 1)$, and so the global ground-state energy satisfies $E^*(m, L) \leqslant mL\epsilon^*(L = 1)$.

Our numerical data suggest this bound to be tight at the leading order in m for any value of L. More precisely, we find numerically that the mean ground-state energy can be very well fitted, for large values of L, by the following formula:

$$\frac{E^*(m, L)}{mL} \simeq -\sqrt{\log(2)} + \frac{A}{m^{3/2}} + \frac{B}{m^{1/2}L}, \tag{19}$$

with $A \sim 0.7$ and $B \sim 0.4$. This behavior clearly shows that the convergence to the asymptotic intensive energy, $-\sqrt{\log(2)}$, becomes faster increasing L: for $L = 1$ corrections are $\mathcal{O}\left(\frac{\log(m)}{m}\right)$ and they become $\mathcal{O}(m^{-3/2})$ in the $L \to \infty$ limit. We see from figure 3 that already for $L \sim 10$, not too close to the boundaries, ground states link energies are independent of L, and their numerical values are well represented by the previous formula with $L = \infty$. Obviously, given the values of m we can study, formula (19) has to be taken as an empirical interpolating function. We find from our data that in ground-state configurations, link energies have very small sample-to-sample fluctuations, which decrease for larger m values: for this reason considering only mean values for the link energies is a good approximation. In order to minimize finite L effects and have a homogeneous ground state inside the window we find that it was enough to consider sister sizes $L = \ell + 20$, i.e. ten sites between the window and system boundaries.

Once understood the ground state structure, let us now turn to the estimate of the window correlation functions.

4.3. Finite m estimates of the correlation functions

Under the assumptions stated above, the weight, in the window partition function, of all the configurations differing in d variables with respect to $\vec{\sigma}^*$ is given by

$$Z_d = (\ell + 1 - d)(2^m - 1)^d \frac{\int_{(d+1)m\epsilon^*}^{\infty} \mathrm{d}z\, \mathrm{e}^{-\beta z - \frac{z^2}{m(d+1)}}}{\int_{(d+1)m\epsilon^*}^{\infty} \mathrm{d}z\, \mathrm{e}^{-\frac{z^2}{m(d+1)}}} \mathrm{e}^{-\beta(\ell-d)m\epsilon^*}, \tag{20}$$

where the first term gives the number of ways to place a bubble of size d in a window of size ℓ, the second term counts the number of configurations of the d variables which have to differ from $\vec{\sigma}^*$, the fraction is the average of $\mathrm{e}^{-\beta H}$ over the pdf of the energies of the bubble (it is the sum of $d+1$ Gaussian variables of variance $m/2$, bounded from below by the ground-state energy, $(d+1)m\epsilon^*$) and the last term is given by the $l - d$ links having the ground-state energy. In equation (20) we have that $d \in \{1, \ldots, \ell\}$, while the weight of the ground state is given by

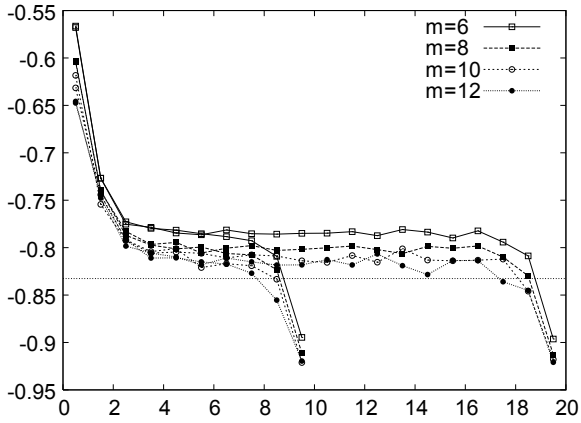

Figure 3. The mean value of the ground-state link energy as a function of the position in the system for $L = 10$ and $L = 20$. On the left boundary the configuration is fixed, while on the right end the system is free. The horizontal line is $-\sqrt{\log(2)}$.

$Z_0 = \exp(-\beta E^*) = \exp(-\beta(\ell+1)m\epsilon^*)$. We do not write explicitly the dependence of Z_d on β, ℓ, m and ϵ^* in order to keep the notation light.

Z_d is an annealed approximation for the window partition function at a fixed distance from the ground state. Still, the fact that we keep the dependence on ϵ^* explicit is important in order to control some fluctuations: e.g. both $\log(p_0)$ and $\log(q_0)$ are given by free-energy differences, where the dependence on ϵ^* is partially canceled out, and their average over ϵ^* can be done without any approximation. The two observables we are interested in are indeed given by

$$p_0 = \frac{Z_0}{\sum_{d=0}^{\ell} Z_d}, \qquad q_0 = \frac{\sum_{d=0}^{\ell}(1-d/\ell)Z_d}{\sum_{d=0}^{\ell} Z_d}, \tag{21}$$

and can be easily computed by evaluating numerically the integrals in the definition of Z_d, once the pdf of ϵ^* is known. We have measured numerically such a distribution, but once we plugged it into equation (20) we discovered that the observables we are interested in ($p_{\rm typ}$ and $q_{\rm typ}$) mainly depend on the mean of ϵ^*, being such a distribution very narrow. Moreover, we are mostly interested in the dependence of these observables on m in order to understand the approach to the $m \to \infty$ limit, and the average of ϵ^* carries the largest dependence on m.

For these reasons, the analytical curves we are going to compare with numerical data in the following section have been obtained using a non-fluctuating value for ϵ^*, give by equation (19) that is $\epsilon^* = -\sqrt{\log(2)} + 0.726/m^{3/2}$. As we show below, this dependence on the interaction range is already enough to produce strong finite m effects. Remind that, in the $m \to \infty$ limit, the logarithm of Z_d is given by the free energy in equation (15), and both $p_{\rm typ}$ and $q_{\rm typ}$ should drop from 1 to 0 when ℓ crosses the value of $\ell_c(\beta)$ given by equation (14).

5. Numerical results

The aim of this section is to compute numerically the above-defined critical length scale for the 1D random energy model. The numerical experiment we have performed consists in

(i) computing the ground state of a system of size L;

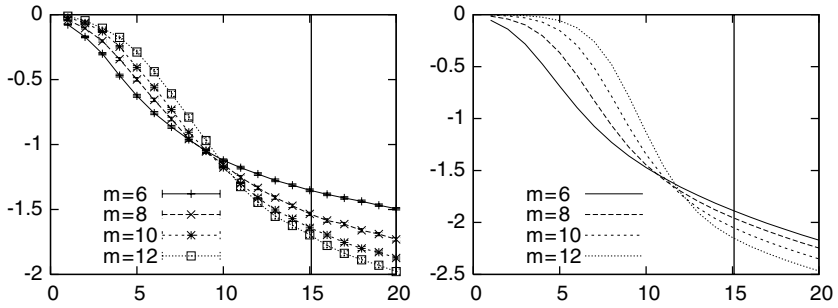

Figure 4. The overlap $q_{\rm typ}$ as a function of ℓ at $T = 0.8$. Left panel: numerical values obtained through the transfer matrix algorithm for various values of m. Right panel: analytic curves obtained through the approximations discussed in the text. The vertical lines mark the value of ℓ_c in the $m \to \infty$ limit.

(ii) fixing the ground-state configuration outside a window of size ℓ;

(iii) computing $q_{\rm typ}$ and $p_{\rm typ}$ in order to see whether there is a first-order transition in these quantities varying the window size ℓ.

In the $m \to \infty$ limit we expect such a transition when the window size crosses the value $\ell_c(\beta)$ given in equation (14). For finite values of m the system cannot have any transition (it is one-dimensional), but still the crossover may be very sharp. Our main interest is in understanding how much the behavior of finite m systems resembles the mean-field (i.e. $m \to \infty$) limit and how fast is the convergence.

As explained in the previous section, we take the size of the system L larger than the size of the window in order to avoid boundary effects; that is, to all practical purposes we are working in the $L \to \infty$ limit.

Thanks to the one-dimensional topology all the experiments can be done exactly by transfer matrix methods. Unfortunately, for each link we have a different random matrix with $2^m \times 2^m$ entries; for this reason we are forced to small values of m (actually we use $m = 6, 8, 10, 12$). Please note that these m values are not so small: the number of degrees of freedom per region (2^m) is comparable or even larger than the number of particles within a typical region studied in realistic models of glassy systems [7]. Since we are interested in computing the free energy at a given value of the overlap with the reference configuration, the transfer matrix computation is slightly more complicated and requires a total time of order $\mathcal{O}(\ell^2 2^{2m})$. The average over the disorder is done with at least 1000 samples for any m value.

We are going to present results for temperature $T = 0.8$, which is a very reasonable value (in the $m \to \infty$ limit the critical temperature is $T_c = 0.600\,56\ldots$), since the critical window size is $\ell_c(T = 0.8) = 15.09$.

In figures 4 and 5 we show, respectively, $\log(q_{\rm typ})$ and $\log(p_{\rm typ})$ as a function of ℓ. Left panels report data from exact numerical computations, while right panels show the outcome of the analytical approximated analysis. The vertical line is the critical window size ℓ_c.

Some comments are in order. The behavior of all the curves for different m hints at a first-order transition for $m \to \infty$ separating a high overlap region at small ℓ from a zero overlap region at large ℓ. This behavior is in agreement with the prediction of the mosaic theory, however, the convergence is very slow! Indeed so slow that it does not allow an estimate of the speed of convergence. The crossing point of numerical data for $\log(q_{\rm typ})$ is around $\ell = 10$, well below the predicted $\ell_c = 15.09$. In principle, one could argue that the

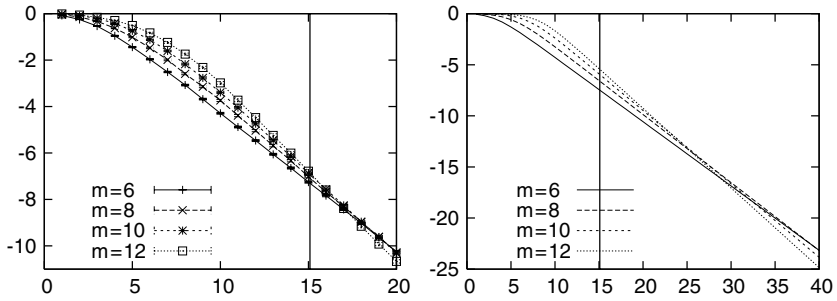

Figure 5. Same as figure 4 for the quantity $p_{\rm typ}$.

one-dimensional model may have a first-order transition at a lower value of ℓ_c, but the crossing point of numerical data for $\log(p_{\rm typ})$, taking place around $\ell = 17$, suggests that the crossing point is strongly dependent on m and converges for $m \to \infty$ somewhere between 10 and 17 (we are assuming that both $q_{\rm typ}$ and $p_{\rm typ}$ have a jump at the same value of ℓ for $m \to \infty$).

Still more evident indications of strong finite m effects come from the analytical curves (see right panels of figures 4 and 5): these have been computed from equations (20) and (21) with $\epsilon^* = -\sqrt{\log(2)} + 0.726 m^{-3/2}$, see equation (19), which is the best interpolation for the ground-state energy in the window, far from the boundaries. Although these curves have been obtained under some approximations, they look qualitatively very similar to the exact numerical data, and also quantitatively are not far from the data. For the analytical curves we know that they have a jump in $\ell = \ell_c$ in the $m \to \infty$ limit, still for the present values of m they show a crossing point quite far from ℓ_c.

Moreover, the value of the overlap at the crossing point may be very small, depending on the overlap one is looking at (see, e.g., the value of $p_{\rm typ}$ at the crossing point). For this reason, it may be very difficult to locate the crossing point (remember that our model has a very strong random first-order transition in the $m \to \infty$ limit, and most probably things work even worst in more realistic models!).

We remark that simulating the model for a single value of m it would be difficult to claim any agreement with the 1RSB theory of glasses and the mosaic state: it is comparing different values on the interaction range m that the agreement becomes apparent. One could argument that one dimension is the worst possibility to observe any behavior reminiscent of a phase transition, and in higher dimension the situation could be more favorable to the theory. Recent simulations of more realistic binary Lennard–Jones mixtures [7], however, failed to identify a sharp mosaic length.

In order to understand better why $q_{\rm typ}$ has such strong finite m corrections and show an effective crossing point at window sizes smaller than ℓ_c, we have studied the window free-energy as a function of the overlap with respect to the ground state. We show in figure 6 such a free energy for $T = 0.8$, $\ell = 10$ and many values of m in order to study the dependence on m. We see that, increasing the value of m, all the curves $f(q)$ tend to decrease, but corrections to the $m \to \infty$ limit are clearly larger for $f(q = 1)$ than for the rest of the curve. Please note that $f(q = 1)$ corresponds to the ground-state energy, that converges in the $m \to \infty$ limit to $-\sqrt{\log(2)}$ (represented by the horizontal line in the plot). The different convergence rate for different q values can be understood also from the analytical computation in the previous section; indeed in the expression for Z_d, see equation (20), larger corrections are for small d values (corresponding to larger q).

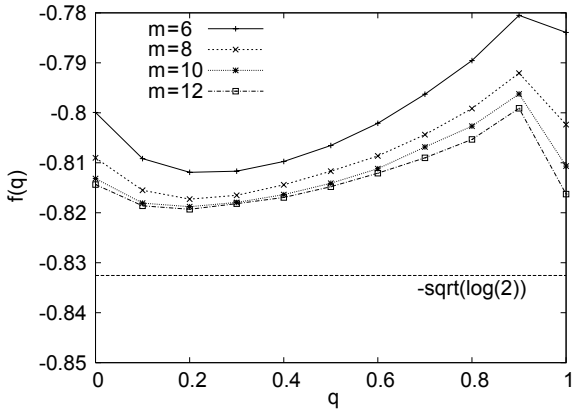

Figure 6. Window free-energy for $\ell = 10$ and $T = 0.8$ as a function of the overlap with respect to the ground-state configuration.

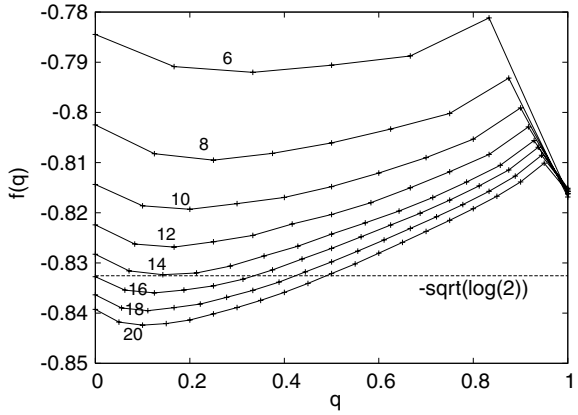

Figure 7. Window free-energy for $T = 0.8$, $m = 12$ and many different values of ℓ, from 6 (top) to 20 (bottom).

A discrepancy with respect to the analytical computation is that the free energy presents a minimum at a positive value of the overlap, while in the $m \to \infty$ limit we expect the minimum to be in $q = 0$. This may be one more effect of the slow convergence to the mean-field limit.

In the tentative of extrapolating the numerical results to the $m \to \infty$ limit, we have fitted $f(q)$ data at fixed q, finding that the limit of $f(q = 1)$ is always compatible with $-\sqrt{\log(2)}$, while for $q < 1$ the asymptotic value of $f(q)$ is quite close to that computed numerically with $m = 12$, especially close to the minimum of $f(q)$.

In figure 7, we show the free energy $f(q)$ for $m = 12$ (which is very close to the $m \to \infty$ value in the low q region) for many ℓ values, ranging from 6 to 20 (top to bottom). The apparent first-order phase transition between the $q = 1$ and the small overlap regimes is taking place between $\ell = 9$ and $\ell = 10$ when the minimum goes below $f(q = 1)$,[4] consistently to what we observe in the left panel of figure 4. Nonetheless, in the $m \to \infty$ we expect the

[4] Please note also that $f(q = 1)$ does not depend on the window size ℓ, confirming that the ground state in the window is insensitive to the boundaries.

transition to take place when the minimum goes below the value $-\sqrt{\log(2)}$, and we see from figure 7 that this happens around $\ell = 14$, much closer to the predicted $\ell_c(T = 0.8) = 15.09$.

6. Conclusions

The scope of this paper is to study the properties of convergence to the mosaic picture in models with larger and larger interaction ranges. We showed that, as should be expected, the behavior of point-to-set correlations approach the behavior predicted by the mosaic picture for large interaction range. The numerical evidence in favor of that comes from a differential analysis comparing the behavior for different values of the interaction range m. Curves at single values of m do not allow us to distinguish the mosaic behavior from a single state picture where the point-to-set correlation exhibit a smooth behavior as a function of ℓ. This is unfortunate as it indicates that it could be difficult to find confirmations or disproval of the mosaic picture in realistic glass former models on the basis of the behavior of point-to-set correlations.

Some papers have recently addressed the study of point-to-set functions in non-disordered models. Amazingly, the model where the mosaic predictions seem to fit better the data is a kinetically constrained model considered in [6] where a step-like behavior of the overlap as a function of the window size is observed. Conversely, for a Lennard–Jones binary mixture, though it is observed a characteristic length growing with temperature, no step behavior is seen. We remark on this purpose that in our data it would be difficult to decide in favor of the mosaic picture on the basis of a single value of m. It is only comparing different values of m that evidence for the first-order jump has been obtained.

Moreover, the convergence to the large m limit is rather slow: finite m curves are very smooth and show no precursor of the asymptotic step-like behavior. In [12], a similar 1D model with a finite interaction range, namely a XORSAT model, is studied. The main difference with respect to our study is that the model studied in [12] possesses zero-energy ground states and has been studied only at zero temperature. Despite these differences also in [12] large finite-range effects have been found.

The main effect that we have seen in the model studied here is that a rather sharp transition takes place at a finite temperature $\beta_c(\ell)$ between a single low-energy ground state (i.e. of zero complexity) and a set of higher free-energy states (with positive complexity) in a way more or less similar to the mosaic picture. However, this transition is plagued by large fluctuations mainly due to the energy of the ground state, which plays a fundamental role in determining the critical temperature: the final effect being a sizable smoothing of the random first-order phase transition at finite value of the interaction range m.

The conclusions reached in this work suggest that the direct observation of the phase transition predicted within the mosaic theory may be rather difficult in realistic models, where the interaction range cannot be made very large. A smarter approach for the identification of such a transition is likely needed.

Acknowledgments

This work was initiated during the workshop ‘Principles of the Dynamics of Non-Equilibrium Systems’, the Isaac Newton Institute for Mathematical Science, Cambridge, 9 Jan–30 Jun 2006. Silvio Franz and Federico Ricci-Tersenghi would like to thank the Newton Institute for the support and the kind hospitality.

References

[1] See Mézard M 2002 *Physica* A **306** 25 for a recent review
[2] Kirkpatrick T R and Wolynes P G 1987 *Phys. Rev.* B **36** 8552
Kirkpatrick T R, Thirumalai D and Wolynes P G 1989 *Phys. Rev.* A **40** 1045
[3] Mézard M and Parisi G 1999 *Phys. Rev. Lett.* **82** 747
[4] Bouchaud J-P and Biroli G 2004 *J. Chem. Phys.* **121** 7347
[5] Montanari A and Semerjian G 2006 *J. Stat. Phys.* **125** 23
[6] Jack R L and Garrahan J P 2005 *J. Chem. Phys.* **123** 164508
[7] Cavagna A, Grigera T S and Verrocchio P 2007 *Phys. Rev. Lett.* **98** 187801
[8] Franz S and Montanari A 2007 *J. Phys. A: Math. Theor.* **40** F251
[9] Franz S and Toninelli F L 2004 *Phys. Rev. Lett.* **92** 030602
Franz S and Toninelli F L 2004 *J. Phys. A: Math. Gen.* **37** 7433
Franz S and Toninelli F L 2005 *J. Stat. Mech.* P01008
[10] Derrida B 1980 *Phys. Rev. Lett.* **45** 79
[11] Brunet E and Derrida B 1997 *Phys. Rev.* E **56** 2597
Brunet E and Derrida B 2001 *J. Stat. Phys.* **103** 269
Brunet E and Derrida B 2004 *Phys. Rev.* E **70** 016106
Brunet E, Derrida B, Mueller A H and Munier S 2006 *Phys. Rev.* E **73** 056126
Brunet E, Derrida B, Mueller A H and Munier S 2007 *Phys. Rev.* E **76** 041104
[12] Montanari A and Sinton A 2007 A simple one dimensional glassy Kac model *Preprint* 0705.0054
[13] Franz S, Parisi G and Ricci-Tersenghi F unpublished